Available online at www.sciencedirect.com
SCIENCE DIRECT®
Biochemical and Biophysical Research Communications 309 (2003) 253–260
BBRC
www.elsevier.com/locate/ybbrc

Comparative proteomics analysis of human lung squamous carcinoma ☆

Cui Li,[a,b] Zhuchu Chen,[a,b,*] Zhiqiang Xiao,[a] Xiaoying Wu,[b] Xianquan Zhan,[b] Xiaopeng Zhang,[b] Maoyu Li,[b] JianLing Li,[a] Xueping Feng,[a] Songping Liang,[c] Ping Chen,[c] and Jing-yun Xie[c]

[a] *Medical Research Center, Xiangya Hospital, Central South University, Changsha 410008, China*
[b] *Cancer Research Institute, Xiangya School of Medicine, Central South University, Changsha 410078, China*
[c] *College of Life Science, Hunan Normal University, Changsha 410006, China*

Received 5 August 2003

Abstract

Two-dimensional polyacrylamide gel electrophoresis (2-DE) profiles of human lung squamous carcinoma tissue and paired surrounding normal bronchial epithelial tissue were compared. Selected differential protein-spots were identified with peptide mass fingerprinting based on matrix-assisted laser desorption/ionization time-of-flight mass spectrometry (MALDI-TOF-MS) and database searching. Well-resolved and reproducible 2-DE patterns of both the tumor and the normal tissues were acquired. The average deviations of spot position were 0.873 ± 0.125 mm in IEF direction and 1.025 ± 0.213 mm in SDS–PAGE direction, respectively. For the tumor tissues, a total of 1349 ± 67 spots were detected and 1235 ± 48 spots were matched with an average matching rate of 91.5%. For the corresponding normal tissues, a total of 1297 ± 73 spots were detected and 1183 ± 56 spots were matched with an average matching rate of 91.2%. A total of 1069 ± 45 spots were matched between the tumor and the normal tissues. Forty differential proteins between tumor and normal tissues were characterized. Some proteins were the products of oncogenes and others were involved in the regulation of cell cycle and signal transduction. These data are valuable for mass identification of differentially expressed proteins involved in lung carcinogenesis, establishing human lung cancer proteome database and screening molecular marker to further study human lung squamous carcinoma.

Keywords: Human lung squamous carcinoma tissue; Normal bronchial epithelial tissue; 2-DE PAGE; MALDI-TOF-MS; Proteome; Differential expression protein

Lung cancer is a malignant tumor with a very high incidence and mortality. According to histological diagnosis, lung cancer comprises a broad spectrum of tumors that include squamous carcinoma, adenocarcinoma, large-cell carcinoma, and small-cell carcinoma. Squamous carcinoma is the most common type, accounting for 30–50% in all of lung cancer patients [1]. Molecular pathogenesis of human lung cancer has been partially revealed at the levels of genomic alteration and transcriptional regulation (mRNA) [2]. However functional complexity of normal and neoplastic tissues is not dictated solely by the encoding genomic information, but also determined by execution molecules, proteins. Thus, the proteomic approach is essential to understand pathogenesis and development of lung cancer. Some tumor-related markers have been identified and are applied in clinic diagnosis thanks to the pioneering proteomic studies. For example, TAO1 and TAO2 are the effective markers that distinguish adenocarcinoma of lung origin from adenocarcinoma metastasized from other organs [3,4]. PGP9.5, a protein that can induce autoantibodies in lung cancer patients [4–6]. Some studies also indicated that AOE372, an antioxidant enzyme, and ATP5D, an ATP synthase subunit, are

☆ *Abbreviations:* 2-DE, two-dimensional polyacrylamide gel electrophoresis; MALDI-TOF-MS, matrix-assisted laser desorption/ionization time-of-flight mass spectrometry; CCA, α-cyano-4-hydroxycinnamic acid; FACS, fluorescence-activated cell sorter; LCM, laser capture microdissection.

* Corresponding author. Fax: +86-731-432-7332.
E-mail address: tcbl@public.cs.hn.cn (Z. Chen).

0006-291X/$ - see front matter © 2003 Published by Elsevier Inc.
doi:10.1016/S0006-291X(03)01578-X

significantly over-expressed in lung adenocarcinoma [7]. These newly identified lung adenocarcinoma specific markers possess great potential in early diagnosis and monitoring responses to therapy. However, these proteomic studies focus on lung adenocarcinoma. A lack of similar study on proteomic profiles of squamous carcinoma hinders our effort to understand and cure this cancer. Therefore, it is necessary to obtain proteomic data on this particular cancer.

2-DE is the principal step of proteomics and widely used in comparative studies of protein expression levels between healthy and diseased states. Hence, in this study, the total proteins from human lung squamous carcinoma and control were separated with 2-DE and analyzed. Differential expression of certain proteins in the tumor and the corresponding normal tissues was revealed by MALDI-TOF-MS and database analysis. The results presented here will no doubt provide clues to further study of the carcinogenic mechanisms, diagnosis, and therapy of lung squamous carcinoma.

Materials and methods

Tissue specimens and preparation. Fifteen human lung squamous carcinoma tissues and paired normal bronchial epithelial tissues adjacent to tumors were obtained from the First and the Second Xiangya Hospital, Central South University. All patients were diagnosed by histopathology. Patients' medical records were reviewed. Fresh tumor tissues and paired tumor-adjacent normal bronchial tissues at least 5 cm away from tumor were obtained immediately after surgery and stored in liquid nitrogen. Epithelial cells were exfoliated from bronchial tissues. The tissues were repeatedly washed with saline in aseptic condition to remove blood and excrescent tissues. Pure population of tumor cells was then scraped from the surface of tumor mass [8]. The processed specimens were either immediately lysed to extract total proteins or were stored at −80 °C until use. A total of 30–80 mg tissues were ground into powder in liquid nitrogen and lysed in 400 μl lysis buffer (7 mol/L urea, 2 mol/L thiourea, 2% NP-40, 1% Triton X-100, 100 mmol/L DTT, 5 mmol/L PMSF, 4% CHAPS, 0.5 mmol/L EDTA, 40 mmol/L Tris, 2% pharmalyte, 1 mg/ml DNase I, and 0.25 mg/ml RNase A). The lysates were vortexed followed by incubation at 37 °C for 1 h. The lysates were centrifuged at 15,000 rpm for 30 min at 4 °C [9]. The supernatant was transferred to a fresh tube and precipitated with TCA sediment method to recover total proteins. The concentration of the total proteins was determined with the BCA Protein Assay Kit (Pierce).

IPG-2D PAGE. IEF was performed using IPGstrip (pH 3-10L, 180 mm × 3 mm × 0.5 mm) on IPGphor isoelectric focusing cell (Amersham Biosciences). Second-dimension SDS–PAGE (Bio-Rad) was conducted as described by manufacturer and Gorg [10]. After electrophoresis, the protein spots were visualized by silver-based staining technique with the protein silver stain kit (Amersham Biosciences).

Image analysis. The stained 2-DE gels were scanned with LabScan software on Imagescanner (Amersham Biosciences). ImageMaster 2D Elite 4.01 analysis software (Amersham Biosciences) was used for spot-intensity calibration, spot detection, background abstraction, matching, 1-D calibration, and the establishment of average-gel. Intensity of each spot was quantified by calculation of spot volume after normalization of the image using the total spot volume normalization method multiplied by the total area of all the spots. The reproducibility of spot position was calculated with Gorbett's method [11]. Statistical analysis was carried out with SPSS for Windows 10.0 and Excel.

MALDI-TOF-MS. Forty differential spots were excised from preparative gels using biopsy punches and transferred to a 1.5 ml siliconized Eppendorf tube. One protein-free gel piece was treated in parallel as a negative control. Proteins were in-gel digested as previously described [12]. The gel-spots were destained in the destaining solution that consisted of 100 mmol/L $Na_2S_2O_3$ and 30 mmol/L $K_3Fe(CN)_6$ (V/V, 1:1). The protein-containing gel-spots were reduced in the reduction buffer (100 mmol/L NH_4HCO_3 and 10 mmol/L DTT) for 1 h at 57 °C and then alkylated in the alkylation buffer (100 mmol/L NH_4HCO_3 and 55 mmol/L iodoacetamide) in the dark for 30 min at room temperature. The gel pieces were dried in a vacuum centrifuge. The dried gel-pieces were incubated in the digestion solution that consisted of 50 mmol/L NH_4HCO_3, 5 mM/L $CaCl_2$, and 0.1 g/L TPCK–trypsin for 24 h at 37 °C. The tryptic peptide mixture was extracted and purified with Millipore ZIPTIP C18 column. The purified tryptic peptide mixture was mixed with CCA matrix solution and vortexed gently. A volume (2 μl) of the mixture containing CCA matrix was loaded on a stainless steel plate and air-dried. The samples were analyzed with Applied Biosystems Voyager System 4307 MALDI-TOF Mass Spectrometer (ABI). The parameters were set up as follows: positive ion-reflector mode, accelerating voltage 20 kV, grid voltage 64.5%, mirror voltage ratio 1.12, N_2 laser wavelength 337 nm, pulse width 3 ns, the number of laser shots 50, acquisition mass range 1000–3000 Da, delay 100 ns, and vacuum degree 4×10^{-7} Torr. A trypsin-fragment peak served as internal standard for mass calibration. A list of the corrected mass peaks was the peptide mass fingerprinting (PMF).

Database analysis. Proteins were identified with peptide mass fingerprinting data by searching software PeptIdent (http://www.expasy.pku.edu.cn). The searching parameters were set up as follows: the mass tolerance was ±0.5 Da; the number of missed cleavage sites was allowed up to 1; the cysteine residue was modified as carbamidomethyl-cys; the minimum number of matched-peptides was 4; species was selected as *Homo sapiens* (human); the peptide ion was $[M + H]^+$; the isotope masses were used; and the searching range was within the experimental p*I* value ±0.5 pH unit and experimental M_r ±20%.

Results

2-DE pattern of human lung squamous carcinoma tissues and normal bronchial epithelial tissues adjacent to tumors

In order to measure the reproducibility, 2-DE for the tumor- and normal-tissues from the same patient was repeated three times, respectively. The image analysis showed that these 2-DE maps were reproducible. A total of 100 well-resolved and matched spots among three tumor-gels were chosen randomly to calculate the deviation of the spot position. The spot positional deviation was 0.873 ± 0.125 mm in the IEF direction and 1.025 ± 0.213 mm in SDS–PAGE direction. For human lung squamous carcinoma tissues, a total of 1349 ± 67 spots were detected, 1235 ± 48 spots were matched with an average matching rate of 91.5%. For normal bronchial epithelial tissues, a total of 1297 ± 73 spots were detected, 1183 ± 56 spots were matched with an average matching rate of 91.2%. The well-resolved and reproducible 2-DE patterns of human lung squamous carcinoma tissues and normal bronchial epithelial tissues

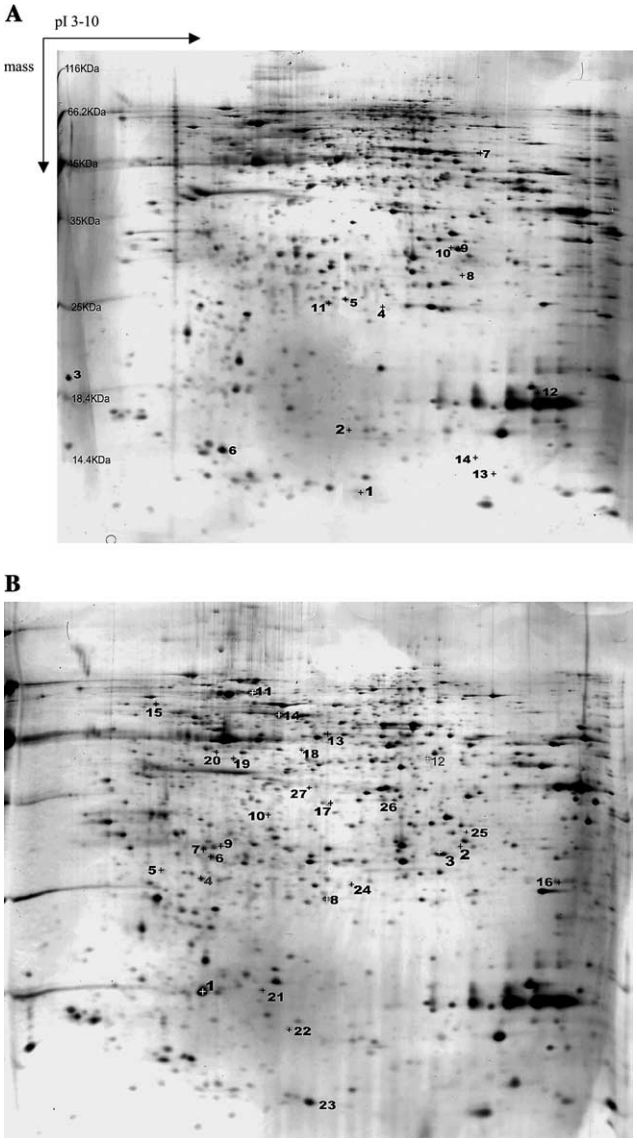

Fig. 1. Two dimensional electrophoretic map of human lung squamous carcinoma tissues and paired tumor-adjacent normal bronchial epithelial tissues. (A) Paired tumor-adjacent normal bronchial epithelial tissues and (B) human lung squamous carcinoma tissues.

adjacent to tumors were attained, which are displayed in Figs. 1A and B. The tumor-2DE maps were compared with the control-2DE maps, a total of 1069 ± 45 spots were matched.

In this study, the 2-DE protein patterns of 15 tumor/normal pairs were quantified and mutually matched. In order to preselect protein variations, the protein patterns of tumor and control tissues were set into two classes and quantities of all detected spots in both classes were compared by Student's *t* test in ImageMaster 2-DE gel analysis software. The 2-DE profiles were very similar among 15 tumor-tissues. To construct a 2-DE map, it is important to have a representative sample. Hence, an average electrophoresis map of human lung squamous carcinoma tissues was constructed by the comparison of the 2-DE maps from 15 tumor-tissues with the ImageMaster 2-DE gel analysis software. The average electrophoresis map included 1942 protein-spots. Similarly, an average electrophoresis map of 15 normal bronchial epithelial tissues was also established with 1853 protein-spots. These average electrophoresis maps were used to perform the differential expression analysis. We compared the 2-DE protein patterns of the average gels of tumor and control tissues, the differential protein-spots between tumor and control tissues with at least fivefold discrepancy were detected in at least five paired tumor- and normal-tissues. Fig. 2 showed differential proteins were found to have a fivefold or greater difference in intensity between tumor and control.

MALDI-TOF-MS PMF analysis of the differential protein-spots

The differential protein-spots between the human lung squamous carcinoma tissues and the paired normal bronchial epithelial tissues were detected by 2-DE gel image analysis software. To determine the accuracy of the matched-result, two matched-spots (N5 and T8) were identified with MALDI-TOF-MS. The results showed that N5 and T8 are the same protein (AC:

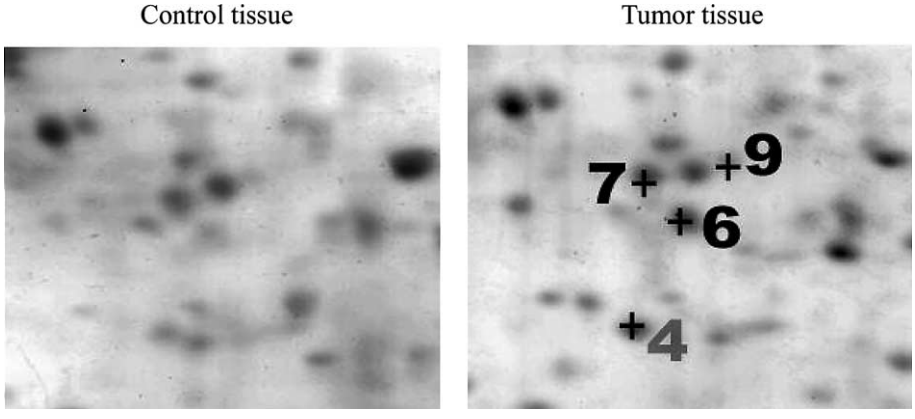

Fig. 2. Differential expression of protein spots up-regulated in tumor tissue.

Table 1
Characterized differentially expressed proteins in human lung squamous carcinoma tissues compared to the paired normal bronchial epithelial tissues adjacent to tumors

Spot number	Expression in carcinoma	Expression in control	Ratio	Peptide matches	AC	Description	p*I*	M_w	Coverage (%)
N1	0	34,510 ± 103		8/50	Q9HC90	Calpain 10 (calcium-activated neutral proteinase 10) (CANP 10)	6.54	15582.85	57.1
N2	0	32,803 ± 217		6/32	P30085	UMP-CMP kinase (cytidylate kinase) (deoxycytidylate kinase) (cytidine monophosphate kinase)	5.44	22222.34	60.2
N3	3043 ± 101	16,785 ± 279	5.52	6/22	Q9BQN3	DJ601O1.1 (novel protein with kunitz/bovine pan creatic trypsin inhibitor domain) (fragment)	Undefined	Undefined	44.2
N4	0	29,743 ± 197		10/61	P36980 (isoform)	SPLICE truncated isoform of complement factor H-related protein 2 precursor (FHR-2) (H factor-like protein 2) (H factor-like 3) (DDESK59)	6.52	27896.58	31.7
N5	71,697 ± 394	14,279 ± 344	5.02	13/47	Q8TCL7	Hypothetical protein (fragment)	Undefined	Undefined	58.1
N6	16201 ± 140	82,953 ± 206	5.12	9/53	P08709	Chain 1: factor VII light chain	5.03	17025.93	65.1
N7	9632 ± 113	54,305 ± 265	5.63	9/44	O60942 (isoform)	SPLICE isoform 3 of mRNA capping enzyme (HCE) (HCAP1) [includes: polynucleotide 5′-triphosphatase (mRNA 5′-triphosphatase) (TPase); mRNA guanylyltransferase (GTP–RNA guanylyltransferase) (GTase)]	8.3	52533.29	22.1
N8	0	23,417 ± 93		8/113	O14753	Putative transcription factor Ovo-like 1 (hOvo1) (fragment)	Undefined	Undefined	36.2
N9	10,352 ± 188	77,843 ± 304	7.52	7/28	Q99871	X-linked protein STS1769	7.22	33582.38	32.2
N10	0	34,875 ± 231		5/18	P09329	Ribose-phosphate pyrophosphokinase I (phosphoribosyl pyrophosphate synthetase I) (PPRibP) (PRS-I)	6.56	34703.04	29.3
N11	10743 ± 184	56,984 ± 195	5.5	14/164	Q14964	Ras-related protein Rab-39	6.9	24869.51	44.2
N12	16825 ± 153	88,631 ± 263	5.27	20/260	Q9NYY1	Chain 1: interleukin-20	8.77	17513.32	63.8
N13	0	19,452 ± 106		4/47	P10073	Krueppel-related zinc finger protein 2 (HKR2 protein) (fragment)	Undefined	Undefined	34
N14	0	21,135 ± 174		9/76	Q01469	Fatty acid-binding protein, epidermal (E-FABP) (psoriasis-associated fatty acid-binding protein homolog) (PA-FABP)	6.6	15164.43	48.1
T1	80789 ± 796	13,687 ± 578	5.9	9/91	Q07812	Apoptosis regulator BAX, membrane isoform α-*Homo sapiens* (human)	5.08	21184.41	57.3
T2	11,100 ± 245	2306 ± 95	48.1	7/32	Q8TDH6	CLL-associated antigen KW-1 splice variant 1 (fragment)	Undefined	Undefined	28.9
T3	76752 ± 678	0		12/31	Q8WW21	Similar to activator of CREM in testis	7.57	32809.7	62.3
T4	55383 ± 376	1189 ± 67	46.58	10/45	P52744	Zinc finger protein 138 (fragment)	Undefined	Undefined	37.2
T5	28379 ± 145	985 ± 43	28.81	11/50	Q9HAV5	Tumor necrosis factor receptor superfamily member XEDAR (X-linked ectodysplasin-A2 receptor) (EDA-A2 receptor)	4.91	32728.66	33.3

T6	42755 ± 745	3506 ± 187	12.19	9/41	Q9NXX7	Hypothetical protein FLJ20001	5.41	33906.7	45.9
T7	53,793 ± 336	4515 ± 246	11.91	8/47	P30279	G1/S-specific cyclin D2	5.06	33067.23	47.4
T8	71697 ± 394	14,279 ± 344	5.02	8/36	Q8TCL7	Hypothetical protein (fragment)	Undefined	Undefined	42.3
T9	29,833 ± 195	0		10/37	Q969U2	Carboxy terminus of HSP70-interacting protein (hypothetical protein) (CLL-associated antigen KW-8)	5.61	34856.2	45.6
T10	25,886 ± 147	0		6/32	P21108	Ribose-phosphate pyrophosphokinase III (phosphoribosyl pyrophosphate synthetase III) (PRS-III)	5.93	34708.13	21.5
T11	70,084 ± 563	6987 ± 241	10.03	32/89	O14985	Mucin 5B precursor (Mucin 5 subtype B, tracheobronchial) (high molecular weight salivary mucin MG1) (sublingual gland mucin)	Undefined	Undefined	24.3
T12	42,124 ± 210	6103 ± 27	6.9	5/16	Q9NZU5	LIM and cysteine-rich domains protein 1 (dyxin)	8.27	40832.79	20.8
T13	27411 ± 184	2046 ± 175	13.4	24/119	Q13422 (isoform)	SPLICE isoform IK7 of DNA-binding protein Ikaros (lymphoid transcription factor LyF-1) -*Homo sapiens* (human)	5.86	52705.82	33.8
T14	74529 ± 403	8503 ± 283	8.77	6/27	P48643	T-complex protein 1, ϵ subunit (TCP-1-ϵ) (CCT-ϵ)	5.45	59671.02	25.7
T15	26942 ± 351	0		22/145	Q12805 (isoform)	SPLICE isoform 3 of EGF-containing fibulin-like extracellular matrix protein 1 precursor (fibulin-3) (FIBL-3) (fibrillin-like protein) (extracellular protein S1-5)	4.95	54583.50	31.7
T16	47673 ± 266	0		27/238	Q13145	CHAIN 1: putative transmembrane protein NMA	8.21	25956.82	71.2
T17	32401 ± 218	0		5/19	076075-2 (isoform)	Splice isoform β of DNA fragmentation factor 40 kDa subunit (DFF-40) (caspase-activated deoxyribonuclease) (caspase-activated DNase) (CAD) (caspase-activated nuclease) (CPAN)	Undefined	Undefined	28.1
T18	29751 ± 350	0		7/24	Z266_HUMAN	Zinc finger protein 266 (zinc finger protein HZF1) (fragment)	Undefined	Undefined	28.5
T19	21,110 ± 109	0		5/24	P18462	Chain 1: HLA class I histocompatibility antigen	5.97	38707.93	28.1
T20	28495 ± 141	5071 ± 153	5.62	6/24	Q00987-5 (isoform)	Splice isoform Mdm2-C of Ubiquitin-protein ligase E3 Mdm2 (p53-binding protein Mdm2) (onco protein Mdm2) (double minute 2 protein) (Hdm2).	4.34	35979.59	40.2
T21	30972 ± 312	0		6/54	Q8NA28	Hypothetical protein FLJ35906.	5.37	20159.17	30.9
T22	26752 ± 104	0		5/41	O14887	Zinc finger protein (fragment)	Undefined	Undefined	87.8
T23	76352 ± 301	14,672 ± 211	5.2	4/34	Q9P003	Protein HSPC163	6.16	16093.36	36.7
T24	30,751 ± 203	0		6/40	Q15933	DNA-binding protein (fragment)	Undefined	Undefined	73.4
T25	29733 ± 104	0		6/35	O43831	NFX.1 (fragment)	Undefined	Undefined	63.2
T26	32181 ± 174	0		6/38	Q8NHD3	SREC-4	6.63	36239.9	39.5
T27	14352 ± 83	2538 ± 39	5.65	8/42	Q15884	Putative protein X123 (fragment)	Undefined	Undefined	34.3

Q8TCL7, hypothetical protein) (Table 1). Forty differential protein-spots (12 spots only expressed in tumor-tissues, seven spots only in control-tissues, the rest of the spots expressed between tumor and control tissues with at least fivefold discrepancy, Table 1) were detected between at least five paired tumor- and control-tissues.

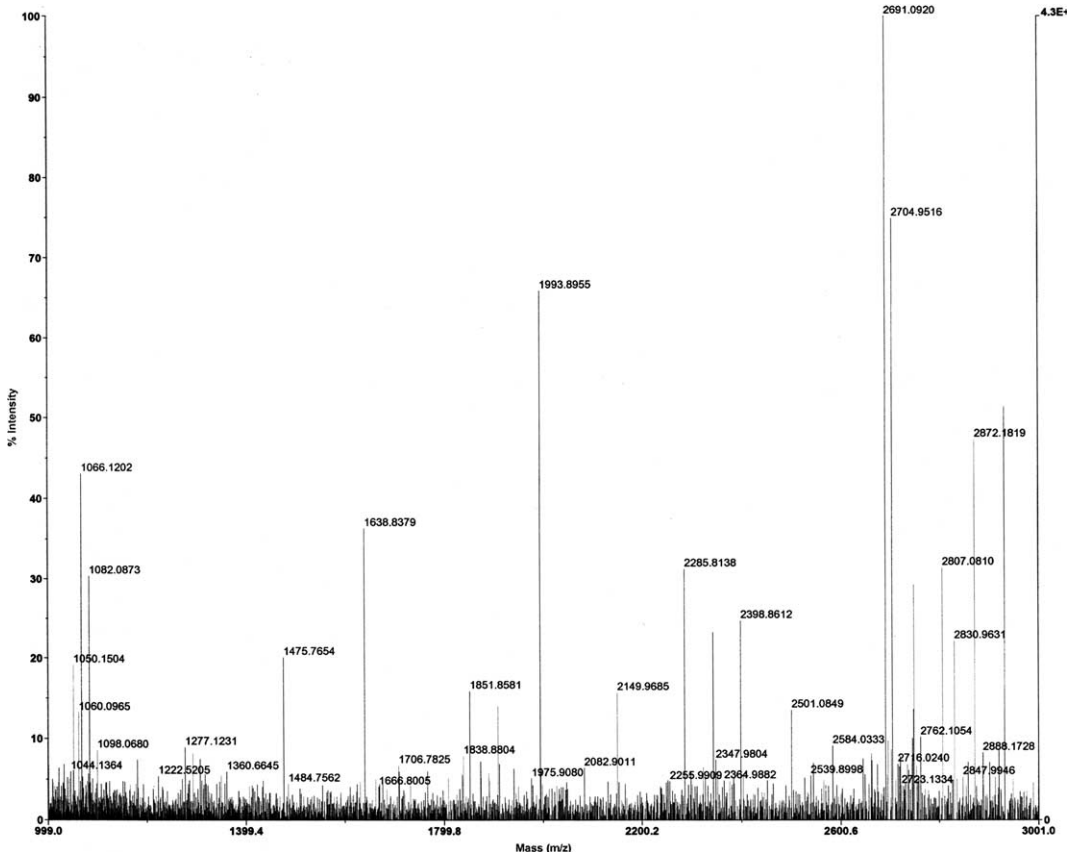

Fig. 3. Peptide mass fingerprinting of protein spot T26 in human lung squamous carcinoma tissues 2-DE map.

Table 2
Matching of protein spot-N11 peptide mass fingerprint data with protein Q14964 in database

User mass	Matching mass	Mass (Da)	#MC	Modification	Position	Peptide
1433.7253	1433.6729	−0.0523	0		182–194	GEICIQDGWEGVK
1490.7519	1490.6944	−0.0574	0	Cys_CAM: 185	182–194	GEICIQDGWEGVK
1692.7992	1692.7278	−0.0713	0	1xCys_CAM, 1xMSO	145–159	LSADCGMMYIETSAK
1708.7766	1708.7227	−0.0538	0	1xCys_CAM, 2xMSO	145–159	LSADCGMMYIETSAK
2238.9573	2239.0964	0.1391	1	Cys_PAM: 41	33–52	FPGLRSPACDPTVGV DFFSR
2262.9988	2262.9927	−0.006	1	1xCys_CAM	140–159	EEAEKLSADCGMMYI ETSAK
2293.1012	2293.0033	−0.0978	1	1xCys_PAM, 1xMSO	140–159	EEAEKLSADCGMMYI ETSAK
2295.1349	2294.9825	−0.1523	1	1xCys_CAM, 2xMSO	140–159	EEAEKLSADCGMMYI ETSAK
2309.0649	2308.9982	−0.0666	1	1xCys_PAM, 2xMSO	140–159	EEAEKLSADCGMMYI ETSAK
2469.1196	2469.321	0.2014	1		1–21	METIWIYQFRLIVIG DSTVGK
2477.007	2477.238	0.231	1		38–60	SPACDPTVGVDFFSR LLEIEPGK
2534.0657	2534.2595	0.1938	1	Cys_CAM: 41	38–60	SPACDPTVGVDFFSR LLEIEPGK
3136.2998	3136.4483	0.1485	1		145–173	LSADCGMMYIETSAK DATNVEESSTILTR
3223.2357	3223.4803	0.2446	1	1xCys_PAM, 1xMSO	145–173	LSADCGMMYIETSAK DATNVEESSTILTR

44.2% of sequence covered:

```
  1        11        21        31        41        51
  |        |         |         |         |         |
  1 METIWIYQFR LIVIGDSTVG Kscllhrftq grFPGLRSPA CDPTVGVDFF SRLLEIEPGK   60
 61 riklqlwdta gqerfrsitr syyrnsvggf lvfditnrrs fehvkdwlee akmyvqpfri  120
121 vfllvghkcd lasqrqvtrE EAEKLSADCG MMYIETSAKD ATNVEESSTI LTRdifdlik  180
181 kGEICIQDGW EGVKsgfvpn tvhpseeavk prkecsc
```

These differential protein-spots were excised from the silver stained gels and digested in-gel with trypsin. The PMF maps were obtained by MALDI-TOF-MS and calibrated with TPCK–trypsin auto-degraded peak ($m/z = 1993.9772$ Da). Fig. 3 showed the PMF maps of the protein-spots T26. The PMF data were used to search the SWISS-PROT and TrEMBL databases with PeptIdent software. The resulting protein was determined by comprehensively considering the corresponding experimental pI, M_r, the number of matched-peptides, and the sequence coverage (Tables 1 and 2). The data on all identified protein spots are described in Table 1, Some proteins were the products of oncogenes, and others were involved in the regulation of cell cycle and signal transduction.

Discussion

The contents of proteomics research, at present, mainly include the establishment of 2-DE reference maps and database from organs, tissues, and cells, and the characterization of special functional proteins by proteomic comparison between healthy and diseased states. The goals of cancer proteomics are to improve molecular classification of tumors and to discover more sensitive biomarkers for disease prognosis and treatment sensitivity prediction.

Our research group has studied the protein expression maps of lung cancer cell lines [13,14]. The obtained protein expression profiles are not reproducible due to the inconsistent time and environment of in vitro cultured cells. In order to establish the protein expression profiles of lung cancer and to characterize the tumor-related proteins, the human lung squamous carcinoma tissues and the paired normal bronchial epithelial tissues adjacent to tumors were analyzed by 2-DE and MS in this study. Due to the complexity and individual difference of human tissues, the 2-DE and subsequent analysis from tissues are far more complex than those from cell line. In this study, the method of surface scraping from tissue is rapid and generally results in pure tumor cell populations, free of contaminating serum proteins, red blood cells, connective tissues, and necrotic tissue materials [8]. If condition permitted, the method such as fluorescence-activated cell sorter (FACS) [15] or laser capture microdissection (LCM) [16] can be employed to obtain pure tumor cells. The protein samples were precipitated in DOC-TCA in order to get rid of high-molecular weight polysaccharides that were abundant in bronchial cartilage, which was not removed from bronchia completely. The well-resolved, reproducible 2-DE profiles from the human lung squamous carcinoma tissues and from the paired normal bronchial epithelial tissues adjacent to tumors were established. The reproducibility of 2-DE profiles was very central to the key point. As variation in experimental procedures is a common source of variability in 2-DE patterns, the generation of reproducible protein maps could be facilitated by the adoption of stringent protocols to ensure uniformity throughout the process. Despite high gel reproducibility, exchange of 2-DE gel patterns for inter-laboratory comparisons should be treated with caution. This is because of some minor variations in sample handling prior to 2-DE and differences in the types of samples. Protocols that may give rise to protein modifications should be avoided, as these changes in sample preparation protocols and handling may result in specific loss or gain of protein species. Compared to Bio-Rad PDQuest 2-DE gel analysis software, the Pharmacia ImageMaster 2D Elite software (4.01 version) had a higher sensitivity. However, the two types of 2-DE gel analysis software all showed time-consuming and labor-consuming. It is necessary to improve their automation degree of analysis. The average gel of lung squamous carcinoma tissues was established by ImageMaster 2D analysis software. The average gel is a statistic synthetic gel of a batch of gels, involving pooling a number of homogeneous samples, which provides more information and improves the accuracy and reliability of analyzed-result [17].

The comparative proteomic study was performed between the human lung squamous carcinoma tissues and the control tissues. Forty differential protein-spots were selected to perform in-gel trypsin digestion and MALDI-TOF-MS-based PMF analysis. Some of the identified proteins with differential expression are the oncogene-encoded products and others are the regulatory proteins of cell cycle and signal transduction. For examples, Cyclin D2, XEDAR (X-linked ectodysplasin-A2 receptor), HSP70-interacting protein (CLL-associated antigen KW-8), Protein HSPC163, p53-binding protein Mdm2, LIM, and cysteine-rich domain protein 1, Ras-related protein Rab-39, and caspase-activated deoxyribonuclease are differentially expressed in both tissues. Niklinski's study showed that Cyclin D is related with carcinogenesis of lung cancer and a potential prognosis marker for non-small cell lung cancer [18]. XEDAR (X-linked ectodysplasin-A2 receptor) is a recently identified member of the tumor necrosis factor receptor family, ligand of which is ectodysplasin-A2 (EDA-A2). XEDAR activates the NF-κB and the JNK pathways in an EDA-A2-dependent fashion and plays a major role in the process of tumor development and progress [19]. MDM2 proto-oncogene expression is aberrant in many human tumors. MDM2 inhibits p53- and p73-mediated cell cycle arrest and apoptosis by binding to transcriptional activation domain of p53 and p73. The N terminus of MDM2 interacts with p53, whereas the C terminus of MDM2 acts on the cyclin A promoter to regulate cell cycle [20]. Heat shock proteins participate in the intracellular dislocation and assembly of

many proteins and are associated with carcinogenesis. LIM and cysteine-rich domain protein 1 may function as regulators of transcription. Altered function of LIM and cysteine-rich domain protein 1 by chromosomal translocations, leads to leukaemia [21]. Our results showed that Cyclin D2, XEDAR, p53-binding protein Mdm2, LIM, and cysteine-rich domain protein 1, HSP70-interacting protein, and protein HSPC163 were up-regulated or expressed only in lung squamous carcinomas, compared to that in normal tissues. These data suggest a role of these proteins in the carcinogenesis of lung squamous carcinoma. Ras-related protein Rab-39 was down-regulated in lung squamous carcinomas compared with control, the mechanism of which awaits further study [22]. The comparative proteomics is an effective platform to study the human lung squamous carcinoma. The 2-DE maps presented in this study will benefit identification of potential tumor markers and understanding of the mechanisms of human lung squamous carcinoma.

Acknowledgments

This work was supported by a grant from National 973 Project of China (2001CB5102), for Outstanding Scholars of New Era from Ministry of Education of China (2002-48), National Natural Science Foundation of China (30000028, 30240056), and key research program from Science and Technology Committee of Hunan, China (02SSY2001-1), and key research program from Public Health Bureau of Hunan Province, China (Z02-04).

References

[1] A.D. Lopez, Counting the dead in China: measuring tobacco's impact in the developing world, BMJ 317 (1998) 1399–1400.
[2] Y. Sekido, K.M. Fong, J.D. Minna, Progress in understanding the molecular pathogenesis of human lung cancer, Biochim. Biophys. Acta 1378 (1998) F21–F59.
[3] T. Hirano, K. Fujioka, B. Franzen, et al., Relationship between TAO1 and TAO2 polypeptides associated with lung adenocarcinoma and histocytological features, Br. J. Cancer 75 (1997) 978–985.
[4] J.M. Oh, F. Brichory, E. Puravs, R. Kuick, C. Wood, J.M. Rouillard, J. Tra, S. Kardia, D. Beer, S. Hanash, A database of protein expression in lung cancer, Proteomics 1 (2001) 1303–1319.
[5] F. Brichory, D. Beer, S. Hanash, et al., Proteomics-based identification of protein gene product 9.5 as a tumor antigen that induces a humoral immune response in lung cancer, Cancer Res. 61 (2001) 7908–7912.
[6] K. Hibi, W.H. Westra, M. Borges, S. Goodman, D. Sidransky, J. Jen, PGP9.5 as a candidate tumor marker for non-small-cell lung cancer, Am. J. Pathol. 155 (1999) 711–715.
[7] G.A. Chen, T.G. Gharib, C.C. Huang, et al., Proteomic analysis of lung adenocarcinoma: identification of a highly expressed set of proteins in tumors, Clin. Cancer Res. 8 (2002) 2298–2305.
[8] A.A. Alaiya, U.J. Roblick, B. Franzen, H.P. Bruch, G. Auer, Protein expression profiling in human lung, breast, bladder, renal, colorectal and ovarian cancers, J. Chromatogr. B 787 (2003) 207–222.
[9] N. Araki, T. Morimasa, T. Sakai, et al., Comparative analysis of brain proteins from P53-deficient mice by two-dimensional electrophoresis, Electrophoresis 21 (2000) 1880–1889.
[10] A. Gorg, C. Obermaier, G. Boguth, et al., The current state of two-dimensional electrophoresis with immobilized pH gradients, Electrophoresis 21 (2000) 1037–1053.
[11] J.M. Gorbett, M.J. Dunn, A. Posch, et al., Positional reproducibility of protein spots in two-dimensional polyacrylamide gel electrophoresis using immobilized pH gradients isoelectric focusing in the first dimension: an interlaboratory comparison, Electrophoresis 15 (1994) 1205–1211.
[12] P. Chen, J.Y. Xie, S.P. Liang, Identification of protein spots in silver-stained two-dimensional gels by MALDI-TOF mass peptide map analysis, Acta Biochim. Biophys. Sin. 32 (2000) 387–391.
[13] X.Q. Zhan, Y.J. Guan, C. Li, Z.C. Chen, J.Y. Xie, P. Chen, S.P. Liang, Differential proteomic analysis of human lung adenocarcinoma cell line A-549 and normal cell line HBE, Acta Biochim. Biophys. Sin. 34 (2002) 50–56.
[14] X.Q. Zhan, Y.J. Guan, Z.C. Chen, C. Li, et al., Analysis of human pulmonary adenocarcinoma cell line NCI-H520 proteome by two-dimensional electrophoresis and MALDI-TOF-MS, Chin. J. Cancer 20 (2001) 575–582.
[15] M. Quadroni, P. James, Proteomics and automation, Electrophoresis 20 (1999) 664–677.
[16] D.K. Ornstein, J.W. Gillespie, C.P. Paweletz, Proteomic analysis of laser capture microdissection human prostate cancer and in vitro prostate cell, Electrophoresis 21 (2000) 2235–2240.
[17] Y.F. Jia, Q.X. Lin, R.J. Guo, H. Guo, S.J. Liu, The image analysis of two-dimensional gel electrophoresis, Prog. Biochem. Biophys. 28 (2001) 246–250.
[18] J. Niklinski, W. Niklinska, J. Laudanski, et al., Prognostic molecular markers in non-small cell lung cancer, Lung Cancer 34 (Suppl. 2) (2001) s53–s58.
[19] S.K. Sinha, S. Zachariah, H.I. Quinones, et al., Role of TRAF3 and -6 in the activation of the NF-kappa B and JNK pathways by X-linked ectodermal dysplasia receptor, J. Biol. Chem. 277 (2002) 44953–44961.
[20] T. Leveillard, B. Wasylyk, The MDM2 C-terminal region binds to TAFII250 and is required for MDM2 regulation of the cyclin A promoter, J. Biol. Chem. 272 (1997) 30651–30661.
[21] I. Sanchez-Garcia, T.H. Rabbitts, LIM domain proteins in leukaemia and development, Semin. Cancer Biol. 4 (1993) 349–358.
[22] G.P. Pfeifer, J.H. Yoon, L. Liu, et al., Methylation of the RASSF1A gene in human cancers, Biol. Chem. 383 (2002) 907–914, legend.